Acta Pharmacologica Sinica (2016) 37: 1190–1198
 1671-4083/16
www.nature.com/aps

Original Article

Over-expressed human TREK-1 inhibits CHO cell proliferation via inhibiting PKA and p38 MAPK pathways and subsequently inducing G_1 arrest

Man ZHANG, Hua-jing YIN, Wei-ping WANG, Jiang LI, Xiao-liang WANG*

State Key Laboratory of Bioactive Substances and Functions of Natural Medicines, Institute of Materia Medica, Chinese Academy of Medical Sciences and Peking Union Medical College, Beijing 100050, China

Aim: Recent studies have shown that the two-pore-domain potassium channel TREK-1 is involved in the proliferation of neural stem cells, astrocytes and human osteoblasts. In this study, we investigated how TREK-1 affected the proliferation of Chinese hamster ovary (CHO) cells *in vitro*.
Methods: A CHO cell line stably expressing hTREK-1 (CHO/hTREK-1 cells) was generated. TREK-1 channel currents in the cells were recorded using whole-cell voltage-clamp recording. The cell cycle distribution was assessed using flow cytometry analysis. The expression of major signaling proteins involved was detected with Western blotting.
Results: CHO/hTREK-1 cells had a high level of TREK-1 expression, reached up to 320%±16% compared to the control cells. Application of arachidonic acid (10 μmol/L), chloroform (1 mmol/L) or etomidate (10 μmol/L) substantially increased TREK-1 channel currents in CHO/hTREK-1 cells. Overexpression of TREK-1 caused CHO cells arresting at the G_1 phase, and significantly decreased the expression of cyclin D1. The TREK-1 inhibitor *l*-butylphthalide (1–100 μmol/L) dose-dependently attenuated TREK-1-induced G_1 phase cell arrest. Moreover, overexpression of TREK-1 significantly decreased the phosphorylation of Akt (S473), glycogen synthase kinase-3β (S9) and cAMP response element-binding protein (CREB, S133), enhanced the phosphorylation of p38 (T180/Y182), but did not alter the phosphorylation and expression of signal transducer and activator of transcription 3 (STAT3).
Conclusion: TREK-1 overexpression suppresses CHO cell proliferation by inhibiting the activity of PKA and p38/MAPK signaling pathways and subsequently inducing G_1 phase cell arrest.

Keywords: TREK-1; CHO cells; G_1 phase arrest; cell proliferation; *l*-butylphthalide; PKA; p38/MAPK

Acta Pharmacologica Sinica (2016) 37: 1190–1198; doi: 10.1038/aps.2016.65; published online 11 Jul 2016

Introduction

Cell proliferation is a vital cellular function and is thus very strictly controlled by several independent mechanisms. It is widely believed that cell proliferation is closely related to potassium channel function, but the roles of these channels in this process are poorly understood. Many studies have demonstrated that numerous potassium channels control cell proliferation, among which Kv1.3 and KCa3.1 are crucial to the regulation of the proliferation of lymphocytes. Additionally, Kv11.1 (HERG), Kv10.1 (Eag1), and K2P 9.1 (TASK-3) have also been found to alter cell proliferation[1].

TREK-1 is a two-pore-domain potassium channel that contributes to background leak K^+ currents and is involved in the regulation of the resting membrane potentials of neurons and other tissues. TREK-1 is expressed throughout the central nervous system (CNS), particularly in the striatum and hippocampus[2]. The widespread expression of TREK-1 in small and medium diameter dorsal root ganglion (DRG) sensory neurons and the preoptic area and anterior hypothalamus makes this background K^+ channel an attractive candidate for a temperature sensor[3].

TREK-1 has been reported to be involved in multiple pathological processes. TREK-1 deficient ($Kcnk2^{-/-}$) mice exhibit a depression-resistant phenotype that mimics treatment with antidepressants[4] . Recently, the expression of TREK-1 has been found to be regulated by fluoxetine in the cortices of depressed animals[5, 6]. Moreover, other studies have demonstrated that TREK-1 activity increases glutamate clearance capability and inhibits inflammatory s100β secretion in cultured astrocytes following hypoxia[7, 8]. Additionally, our previous studies have demonstrated that both the mRNA and protein levels of TREK-1 were increased at 2 h after middle

*To whom correspondence should be addressed.
E-mail wangxl@imm.ac.cn
Received 2015-12-31 Accepted 2016-04-22

cerebral artery occlusion in the cortex and hippocampus[9]. Furthermore, in a long-term study using the above mentioned pathological model, the expression of TREK-1 significantly increased at d 3, 7, and 30 after the operation[10, 11]. Therefore, TREK-1 is involved in various cell functions, and it may become potential drug target for the treatment of CNS diseases.

Recently, some studies have found that TREK-1 may influence cell cycle progression. Up-regulation of TREK-1 at both the protein and mRNA levels leads to decreased neuronal stem cell (NSCs) proliferation that can be reversed with bupivacaine treatment. These findings indicate that TREK-1 may be involved in NSC proliferation after focal ischemia[5]. Several studies have demonstrated that TREK-1 inhibits both astrocyte proliferation under hypoxic conditions[10] and human osteoblasts proliferation[12]. We have previously found a negative relationship between TREK-1 expression and heart development in newborn rats and that the proliferation of normal and hypoxia-injured cardiac myocytes is induced by shRNA silencing of the TREK-1 gene[13]. However, some studies have demonstrated the opposite results. Voloshyna[14] and colleges demonstrated that the overexpression of TREK-1 increases the proliferation of prostate cancer cell lines. Therefore, the action and mechanisms of TREK-1 that influence cell proliferation remain unclear.

In the present study, we constructed a Chinese hamster ovary (CHO) cell line that stably expresses the human TREK-1 channel and investigated the effects of TREK-1 overexpression on proliferation. Specifically, we investigated the signaling pathways involved in this process and the effects of a TREK-1 inhibitor on cell proliferation.

Materials and methods

Plasmid construction

The following human KCNK2 variant a (NCBI Reference Sequence: NM_001017424, 422 amino acids)-specific primers containing *Sac* I or *Kpn* I sites were used: forward, 5′-AAGAGCTCCAAATGATGAACCCACGAGC-3′; and reverse, 5′-GGGGTACCGGCTCTTTGATGTTCTCAATC-3′. The PCR reaction mixes contained 10.0 μL 5× PCR buffer (Mg^{2+} plus), 1.0 μL dNTPs (10 mmol/L), 1.0 μL of each primer (10 μmol/L), 4.0 μL template cDNA, and 0.5 μL Phusion® High-Fidelity DNA polymerase (2 U/mL) (New England Biolabs, Hitchin, Herts, UK), and double distilled water was added to a total volume of 50 μL. The PCR reaction included pre-denaturation at 98 °C for 30 s and 35 amplification cycles each consisting of denaturation at 98 °C for 10 s, annealing at 65 °C for 30 s, and extension at 72 °C for 2 min. The PCR products were separated by electrophoresis on 1% ethidium bromide-stained agarose gel and visualized under UV light. The target fragment was purified with a gel extraction kit (TIANGEN, Beijing, China), and the PCR products and pEGFP-N1 vector were then digested with *Sac* I and *Kpn* I restriction enzymes. The digested pEGFP-N1 vector was ligated with the insert KCNK2 variant a cDNA with T4 DNA ligase to generate the eukaryotic expression vector pEGFP-N1-hTREK-1a. The recombinant vector was amplified in *E coli* DH5α and then extracted with a Qiagen Maxi plasmid kit (Qiagen, CA, USA). In the following experiments, the hTREK-1a-expressing CHO cell line was used.

Cell culture and transfection

The CHO cells were cultured in DMEM (Gibco, CA, USA) supplemented with 10% FBS (HyClone, UT, USA). The cells were grown at 37 °C in a humidified atmosphere containing 5% CO_2 and subcultured approximately every 3 d. When the CHO cells grew to 75%–80% confluence, the transfections were performed. Using MegaTran 1.0 transfection reagent (Origene, Beijing, China), the pEGFP-N1/hTREK-1a plasmid was transfected into the CHO cells. Fresh medium containing 0.8 mg/mL G418 was supplied to the transfected CHO cells 24 h after transfection, and a cell pool was obtained after 2 weeks of selection.

Electrophysiology

The membrane currents were recorded in the whole-cell voltage clamp configuration. Glass recording pipettes with resistances of 3–5 MΩ were used. The external solution contained the following (in mmol/L): NaCl, 150; KCl, 5.4; $MgCl_2$, 2; $CaCl_2$, 1.2; glucose, 15; and HEPES, 5 (titrated to pH 7.4 with NaOH). The patch pipette solution contained the following (in mmol/L): KCl, 140; $MgCl_2$, 0.5; EGTA, 10; and HEPES, 10 (titrated to pH 7.2 with KOH). Currents were evoked in response to voltage ramps, and voltage steps were generated using an EPC-10 patch-clamp amplifier (HEKA Electronics, Lambrecht, Germany). The data were analyzed using Pulse 8.6 software (HEKA Electronics, Lambrecht, Germany). Before seal formation, the voltage offset between the patch electrode and the bath solution was adjusted to produce zero current. After seal formation (≥1 GΩ) and membrane rupture, the cells were allowed to stabilize for approximately 5 min. The holding potential during the experiments was set to -80 mV. All of the electrophysiological measurements were performed at room temperature (23–25 °C).

Flow cytometric analysis of the cell cycle distribution

The protocol for the cell cycle analysis was that of the CyStain DNA 1 step kit (Partec, Munster, Germany). Briefly, the cells were seeded at 5×10^4 cells/well in 6-well plates. Twenty-four hours after seeding, fresh complete medium containing *l*-NBP (3-*n*-butylphthalide; 10, 30, and 100 μmol/L) or DMSO vehicle was added, and after 48 h of treatment, the CHO cells were trypsinized, centrifuged, and resuspended in 5 mL of PBS. The cells were spun down again, and the PBS was removed. One milliliter of CyStain DNA 1 step was added to the pellet, which was then vortexed and incubated for 5 min at room temperature. The sample was filtered through a 50-μm cell strainer and detected by flow cytometry with a Partec flow cytometer, and the data were analyzed with FCS Express software.

Western blot analysis

The CHO cells were collected and lysed in cell lysis buffer containing a protease inhibitor cocktail (Roche). The cells were pelleted by centrifugation at 4 °C for 30 min at 12000×*g*, and the supernatants were boiled for 5 min and stored at -20 °C. Equal amounts of proteins (30 μg) were loaded on a 10% SDS-PAGE gel, and the gel was wet-transferred onto PVDF membranes. The membranes were blocked with TBS buffer containing 5% non-fat milk for 2 h and subsequently incubated at 4 °C overnight in buffer containing mouse anti-β-actin (1:10000, Sigma-Aldrich, MO, USA, A5441), rabbit anti-TREK-1 (1:1000, Novus, CO, USA, NB110-41535), rabbit anti-cyclin D1 (1:1000, Cell Signaling Technology, MA, USA, 2978), rabbit anti-p-Akt (Thr 308, 1:1000, Cell Signaling Technology, MA, USA, 9275), rabbit anti-p-Akt (Ser 473, 1:1000, Cell Signaling Technology, MA, USA, 9278), rabbit anti-Akt (1:1000, Cell Signaling Technology, MA, USA, 9272), rabbit anti-p-GSK-3β (Ser 9, 1:1000, Cell Signaling Technology, MA, USA, 5558), rabbit anti-GSK-3β (1:1000, Cell Signaling Technology, MA, USA, 5676), rabbit anti-p-STAT3 (Tyr 705, 1:2000, Cell Signaling Technology, MA, USA, 9145), rabbit anti-STAT3 (1:2000, Cell Signaling Technology, MA, USA, 4904), rabbit anti-PKA (1:50000, Novus, CO, USA, NBP1-95243), rabbit anti-p-CREB (Ser 133, 1:1000, Cell Signaling Technology, MA, USA, 9198), rabbit anti-CREB (1:1000, Cell Signaling Technology, MA, USA, 9197), rabbit anti-p-p38 (Thr 180/Tyr 182, 1:500, Cell Signaling Technology, MA, USA, 9212), or rabbit anti-p38 (1:500, Cell Signaling Technology, MA, USA, 7973). The membranes were washed three times and subsequently incubated with goat anti-rabbit IgG HRP (1:10000) or rabbit anti-mouse IgG HRP (1:10000) in TBST at room temperature for 1 h. The same membranes were immunoblotted against β-actin for data normalization. The immunoreactive proteins were visualized with an LAS-3000 imager (FUJIFILM, Tokoyo, Japan), and the band intensities were quantified with Quantity One software (BioRad Life Science, Hercules, CA, USA).

Statistical analysis

GraphPad Prism version 5.0 was used to analyze the data. All data are expressed as the mean±SEM. The flow cytometric and Western blot data were analyzed with unpaired two-tailed Student's *t*-tests, and the electrophysiological data were analyzed with paired two-tailed Student's *t*-tests. Values of $P<0.05$ were considered statistically significant.

Results

Expression and electrophysiological characteristics of the TREK-1 channels

To study the biological functions of TREK-1, we generated a recombinant plasmid containing TREK-1 and transfected this plasmid into CHO cells (described above). After two weeks of culture in the presence of 0.8 mg/mL G418, a resistant cell pool was obtained. Cells transfected with pEGFP-N1 were used as controls (termed CHO/EGFP cells).

We performed Western blot to detect and verify the expression of TREK-1 in the transfected CHO cells. The CHO/hTREK-1 cells exhibited high levels of TREK-1 expression, whereas none of the controls yielded any visible bands. The value of the control group was taken as 100%, and the expression of TREK-1 in the CHO/hTREK-1 cells reached up to 320%±16% ($P<0.01$).

In the CHO/EGFP cells, a diffuse cytosolic EGFP labeling was present (Figure 1A and 1B), whereas the majority of the EGFP was localized to the membrane surface in the CHO/hTREK-1 cells (Figure 1C and 1D). However, we and other groups have found that TREK-1 is substantially expressed in the nucleus[14]. Therefore, further studies are required to determine the significance of TREK-1 expression in the nucleus.

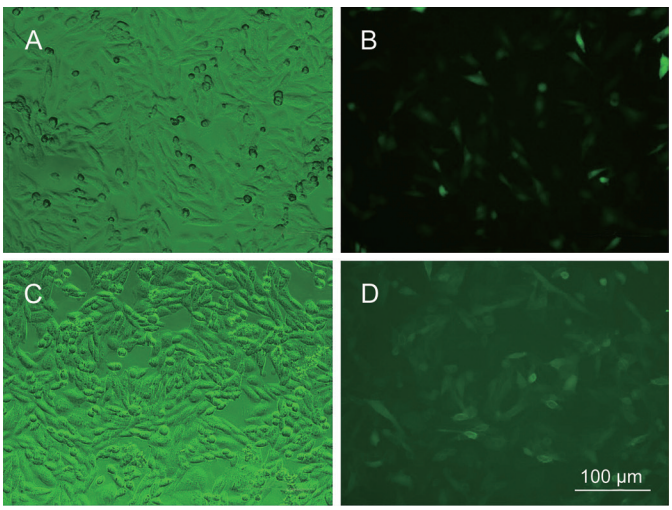

Figure 1. Expression of EGFP or TREK-1 protein in the CHO cells. Typical pictures of cells stably transfected with the pEGFP-N1 control plasmid observed with transmission (A) and fluorescence microscopy after G418 selection for 2 weeks (B). Typical picture of cells stably transfected with the pEGFP-N-hTREK-1a plasmid observed with transmission (C) and fluorescence microscopy after G418 selection for 2 weeks (D). Scale bar, 100 μm.

Polyunsaturated fatty acids and inhalational anesthetics have the ability to increase the activities of TREK-1 channels[15, 16]. Thus, we measured the activity of the TREK-1 channel expressed on the CHO/hTREK-1 cells using arachidonic acid (AA), chloroform ($CHCl_3$) and etomidate. As expected, 10 μmol/L AA, 1 mmol/L $CHCl_3$, and 10 μmol/L etomidate substantially increased TREK-1 activity. The TREK-1 current was measured at the end of a voltage clamp pulse in the patch-clamp whole-cell recording mode. AA at 10 μmol/L increased the currents from 401±90 pA to 685±117 pA (Figure 2A and 2B), $CHCl_3$ at 1 mmol/L increased the currents from 456±77 pA to 752±91 pA (Figure 2C and 2D), and etomidate at 10 μmol/L increased the currents from 405±154 pA to 649±202 pA (Figure 2E and 2F) after depolarization from -80 mV to +60 mV. For convenience, we used enhanced green fluorescence protein (EGFP) as a tag, and our data revealed that the properties of the channel were unaltered by the presence of EGFP,

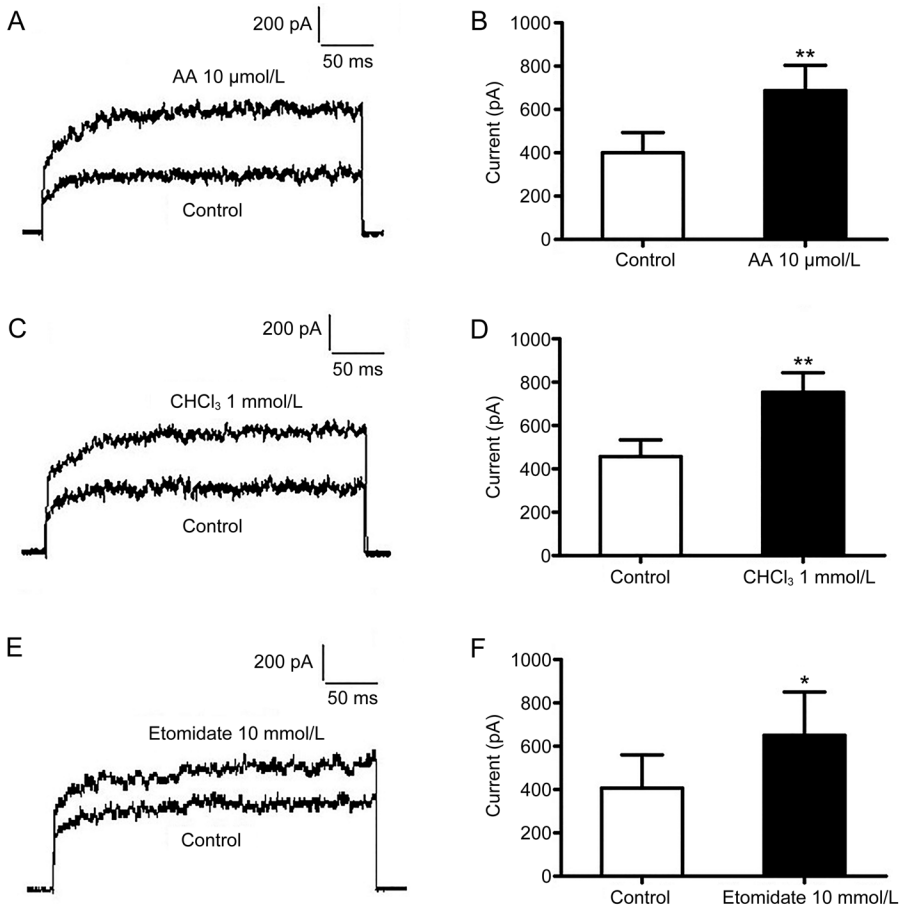

Figure 2. TREK-1 channel currents were activated by 10 μmol/L AA, 1 mmol/L $CHCl_3$ and 10 μmol/L etomidate. (A, B) The TREK-1 currents were measured at +60 mV, and they increased from 401±90 pA to 685±117 pA after 10 μmol/L AA was applied (n=5). (C, D) The TREK-1 currents were measured at +60 mV, and they increased from 456±77 pA to 752±91 pA after 1 mmol/L $CHCl_3$ was applied (n=5). (E, F) The TREK-1 currents were measured at +60 mV, and they increased from 405±154 pA to 649±202 pA after 10 μmol/L etomidate was applied (n=4). Each bar presents the mean±SEM, and the data were analyzed with paired two-tailed Student's t-tests. $^{*}P<0.05$, $^{**}P<0.01$ compared with the control CHO/EGFP cells.

results consistent with those from a previous study[12]. Hence, the CHO cells expressing human TREK-1 could be used to study the function of the TREK-1 channel.

TREK-1 overexpression inhibited the transition from the G_1 to the S phase in TREK-1 transfected cells, and this effect was reversed by *l*-NBP

To evaluate the biological function of TREK-1 in proliferation, we used flow cytometry analyses to measure the cell cycle distributions of CHO/hTREK-1 and CHO/EGFP cells. The results indicated that human TREK-1 overexpression inhibited CHO cell proliferation. The percentage of the CHO/hTREK-1 cells entering the G_1 phase was 59.3%±2.6% (Figure 3B), which was higher than that in the CHO/EGFP cells (46.2%±0.3%, Figure 3A, $P<0.01$), and resulted in a corresponding decrease in the number of cells in the G_2/M phase ($P<0.01$). Thus, these results suggest that TREK-1 might inhibit CHO cell growth by inhibiting the G_1 to S phase transition in the cell cycle.

Because the overexpression of TREK-1 inhibited CHO cell proliferation as demonstrated above, we next determined whether suppressing its activity would reverse the effect of TREK-1 on proliferation. The potent neuro-protectant 3-*n*-butylphthalide (NBP) was approved by the Food and Drug Administration of China (CFDA) at the end of 2002 as a new drug for the treatment of ischemic stroke, and NBP inhibits TREK-1 currents[17, 18]. Additionally, our previous study has demonstrated that the optical isomer *l*-NBP inhibits TREK-1 currents more potently than the dl- and d-NBP isomers, and *l*-NBP decreases the expression of TREK-1[19, 20]. Therefore, we used the *l*-NBP as a TREK-1 inhibitor. As illustrated in Figure 3C, after 72 h of *l*-NBP treatment, the number of cells in the G_1 phase was significantly decreased compared with the CHO/hTREK-1 cell control group. The cell numbers in the G_1 phase in the *l*-NBP groups the received 1, 3, 10, 30, and 100 μmol/L were 60.0%±0.3%, 59.6%±0.2%, 57.3%±0.2%, 53.3%±0.7%, and 42.5%±1.9%, respectively. These results suggested that TREK-1 inhibited the proliferation of CHO cells, however, the specific TREK-1 blocker *l*-NBP reversed the inhibitory effect of TREK-1 on cell proliferation. Consistently with the flow cytometry results, after *l*-NBP treatment (at 1, 50, and

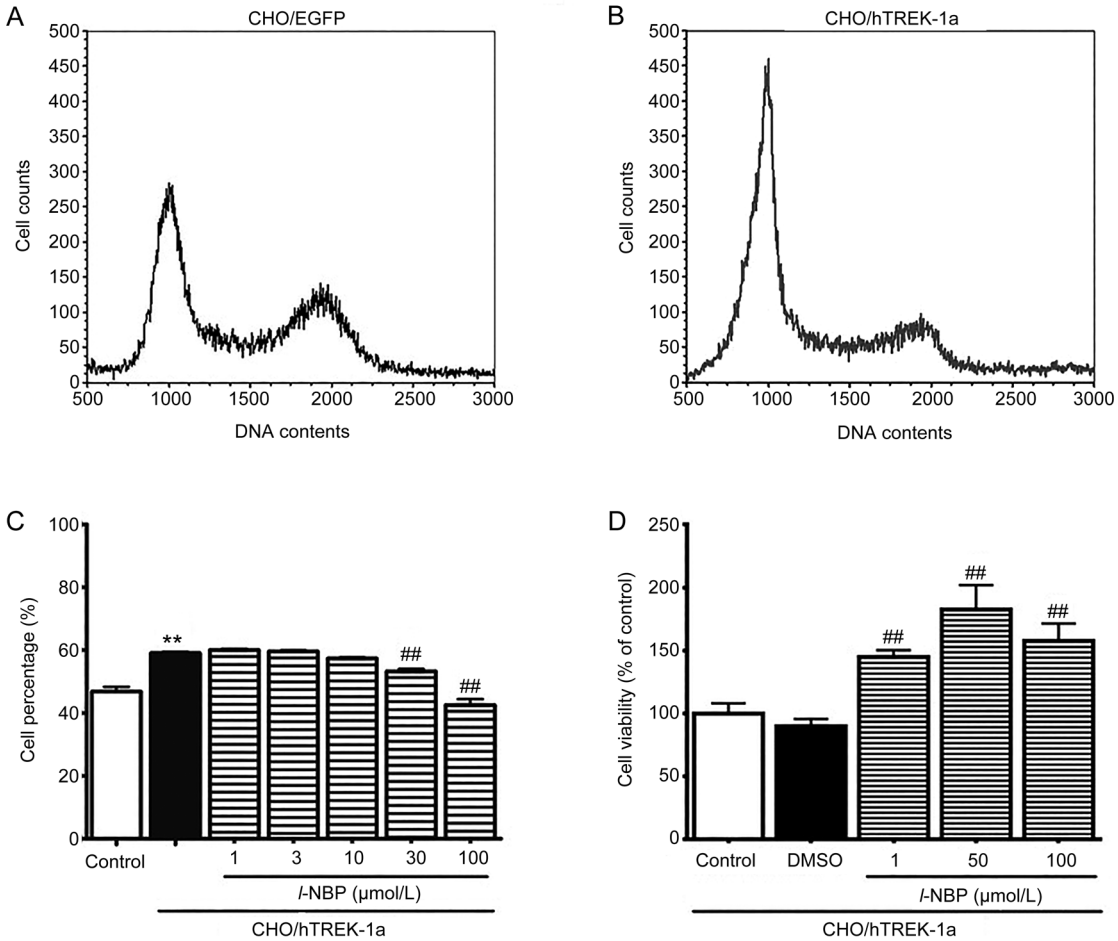

Figure 3. TREK-1 increased the percentage of cells in the G_1 phase, and *l*-NBP reversed the effect of TREK-1 on the cell cycle distribution. The cell cycle analyses of the CHO cells transfected with the pEGFP-N1 plasmid (A) or the pEGFP-N-hTREK-1a plasmid (B). (C) *l*-NBP increased the proliferation of the CHO/hTREK-1a cells. The columns indicate the mean numbers of cells in the different phases of the cell cycle as determined with FCS express 4 Flow, Research Edition. (D) *l*-NBP increased the viability of the CHO/hTREK-1a cells. The bars indicate the SEM. These results were typical of three independent experiments, n=3. $^{**}P$<0.01 compared with the control CHO/EGFP cells, and $^{\#\#}P$<0.01 compared with the model CHO/hTREK-1a cells.

100 μmol/L), the cell viabilities were significantly increased compared with the control group according to MTT assays (Figure 3D, P<0.01).

Cyclin D1 is down-regulated in TREK-1-overexpressing cells

To understand the molecular mechanisms of the effects of TREK-1 on cell proliferation, we detected the expression of cyclin D1 in the cells (Figure 4). Cyclin D1 is central to cell cycle arrest, the up-regulation or overexpression of cyclin D1 shortens the G_1 period, and cyclin D1 has been found in a variety of cancers[21–25]. The relative level in the control was taken 100%, and consistently with the cell cycle distributions, the levels of cyclin D1 decreased to 64.9%±6.8% in the TREK-1-overexpressing cells (P<0.01).

Reduced cyclin D1 expression due to decreased PKA and AKT signaling and CREB activity

To further investigate the mechanism by which TREK-1 reduced the expression of cyclin D1 and inhibited cell proliferation, the phosphoinositide 3-kinase (PI3-K)/Akt signaling pathway, the cAMP-dependent protein kinase A (PKA)/cAMP response element binding protein (CREB) pathway, the Janus kinases (JAK)/signal transducer and activator of transcription (STAT) pathway and the mitogen-activated protein kinases (MAPK) pathway were examined (Figures 4 and 5).

Western blot analysis of the phosphorylated Akt (p-AKT) levels indicated that the Akt activity was decreased in the CHO/hTERK-1 cells compared with the CHO/EGFP cells (Figure 4). In the CHO/hTREK-1 cells, the phosphorylation of Akt at Ser 473 was decreased to 71.7%±5.9% (Figure 4, P<0.05), and no obvious changes in Akt phosphorylated at Thr 308 or the total Akt protein levels were observed, which demonstrated that TREK-1 decreased the activity of Akt by inhibiting the phosphorylation of Akt at Ser 473 rather than Thr 308 but had no effect on protein stability. In agreement with the decrease in the phosphorylation of Akt in the CHO/hTREK-1 cells, the phosphorylation of glycogen synthase kinase-3β (GSK-3β) at the Ser 9 site was down-regulated to 70.4%±11.0%

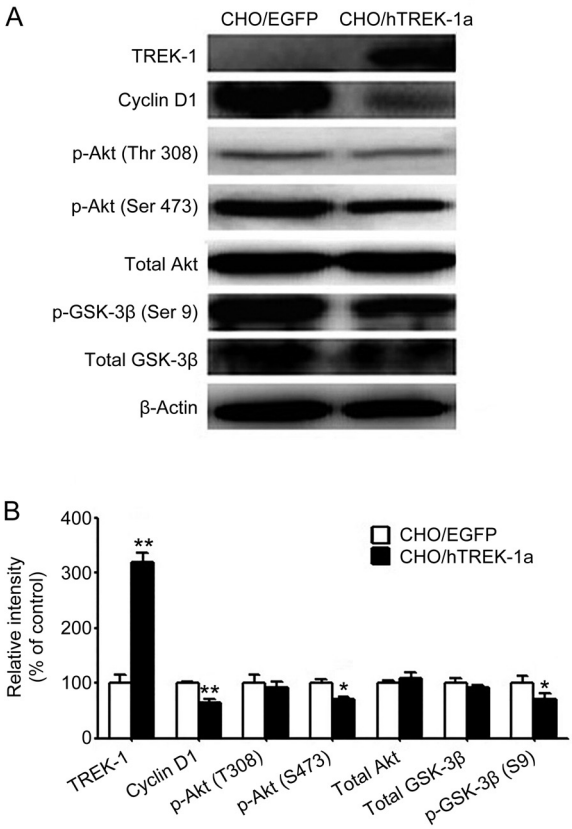

Figure 4. TREK-1 inhibited the expression of cyclin D1 by inhibiting the PI3K/Akt signaling pathway. (A) Western blot analyses of the expression of TREK-1, cyclin D1, and the expression and phosphorylation of Akt and GSK-3β in CHO cells transfected with the pEGFP-N1 or pEGFP-N-hTREK-1a plasmid. (B) The bands were analyzed using the Quantity One software. Each bar corresponds to the mean±SEM. These results were typical of three independent experiments, n=3. $^{*}P$<0.05, $^{**}P$<0.01 compared with the control CHO/EGFP cells.

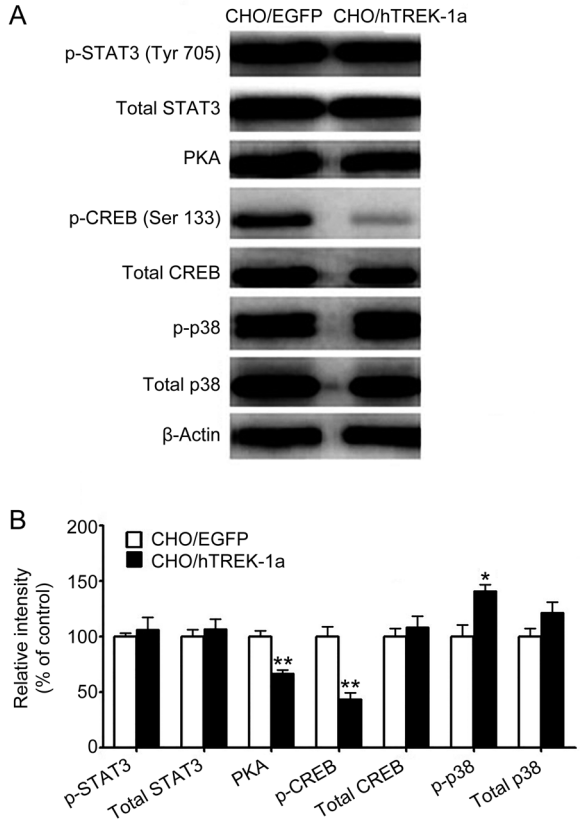

Figure 5. TREK-1 inhibited the PKA/CREB pathway, activated the p38 MAPK signal pathway, and had no obvious influence on the JAK/STAT pathway in CHO cells. (A) Western blot analyses of the expression and the phosphorylation of CREB and p38 and the expressions of the PKA catalytic subunits. (B) The bands were analyzed using Quantity One software. Each bar corresponds to the mean±SEM. These results were typical of three independent experiments, n=3. $^{*}P$<0.05, $^{**}P$<0.01 compared with the control CHO/EGFP cells.

(Figure 4, P<0.05), and no significant change in total GSK-3β was observed.

We also examined the effect of TREK-1 on the PKA/CREB pathway. Ser133 as a key regulatory site that must be phosphorylated for CREB to stimulate the expressions of target genes. In the TREK-1 cells, the level of the PKA catalytic subunit was decreased to 66.7%±3.2% (Figure 5, P<0.01). Consistently with this result, the phosphorylation of CREB at Ser 133 was significantly decreased to 44.0%±5.7% (Figure 5, P<0.01), whereas no obvious change in total CREB protein was observed.

In addition to the PKA/CREB and Akt signaling pathways, the p38 MAPK pathway also regulates cell cycle progression at different transition points by both transcription-dependent and transcription-independent mechanisms[26]. Therefore, we detected the expression and phosphorylation of the p38 protein. Compared with the control group, the phosphorylation of the p38 protein was significantly increased to 141.2%±5.9% (P<0.05), whereas its expression exhibited no obvious change (Figure 5).

Next, we assessed whether other signal pathways led to the down-regulation of cyclin D1. We also examined the effect of TREK-1 on the JAK/STAT pathway, and there were no obvious changes in the expression or phosphorylation of STAT3. These results indicated that STAT3 is not involved in the process of diminishing the expression of cyclin D1 (Figure 5).

Discussion

In the present study, we constructed a CHO cell line that stably expressed the TREK-1 channel and studied the effects of TREK-1 on cell proliferation and the relevant signal pathways. Previous studies have indicated that enhanced expression of the mRNA and protein of TREK-1 by TREK-1 gene transfection suppresses the growth of NSCs and COS7 cells[5, 12]. Highly expressed TREK-1 might also inhibit the proliferation of astrocytes. Fluoxetine, which is a TREK-1 blocker, has also been found to inhibit the reduction in cell proliferation[27, 28]. In agreement with these reports, in the present study, we found that the overexpression of TREK-1 inhibited cell prolifera-

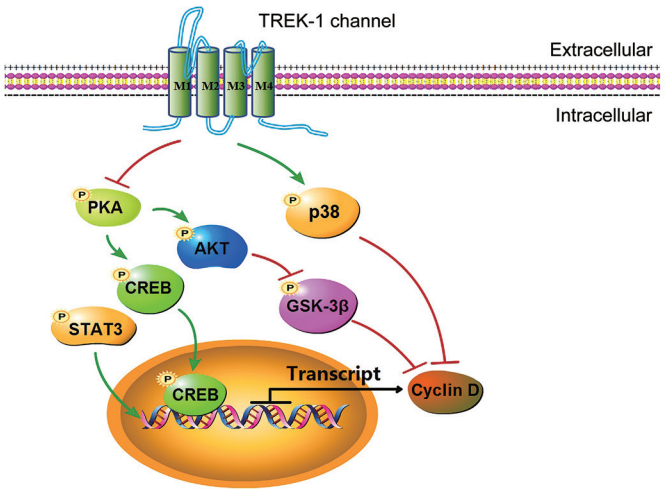

Figure 6. Schematic diagram of the signaling pathways through which TREK-1 inhibits cell proliferation. TREK-1 inhibits the activity of PKA and then reduces the phosphorylations of CREB and Akt, which result in the inhibition of the expression of cyclin D1 and the induction of the degradation of cyclin D1, respectively. Therefore, CHO cell proliferation was inhibited due to the decrease in cyclin D1. TREK-1 increased the phosphorylation of p38, which also inhibited the expression of cyclin D1.

tion by attenuating the G_1/S transition and that the TREK-1 blocker *l*-NBP promoted the proliferation of the TREK-1 overexpressing cells.

According to our finding that G_1 is arrested by increased TREK-1 expression, we detected the expression of cyclin D1, which is a critical target of proliferative signals in G_1 phase. Cyclin D1 forms activating complexes with CDK4 and CDK6 that phosphorylate retinoblastoma tumor-suppressor protein (Rb) and prevent the binding of Rb with the E2F family, which activates the transcription of the cyclin E and thereby initiates the G_1/S transition[29, 30]. Our results indicated that reduced cyclin D1 expression in the CHO/hTREK-1 cells led to inhibition of the proliferation these cells and specifically increased the percentage of cells in G_1 phase.

Many kinases and signaling pathways in the cell cycle are involved in controlling the level of cyclin D1. β-Catenin, CREB and STAT promote the transcription of cyclin D1, Akt increases the translation of cyclin D1, and GSK-3β, which is a downstream target of Akt, regulates the proteasomal degradation of cyclin D1[31]. Additionally, the expression of cyclin D1 is also down-regulated by p38[32]. We demonstrated that the overexpression of TREK-1 in the CHO/hTREK-1 cells resulted in the down-regulation of phosphorylated Akt, GSK-3β, and CREB as well as a reduction in the level of the PKA catalytic subunit. The overexpression TREK-1 also enhanced phosphorylated p38, whereas no obvious changes were observed in total or phosphorylated STAT3.

It has been suggested that TREK-1 interacts with A-kinase-anchoring proteins (AKAPs) and MAP2[33]. PKA regulatory subunit type II (RII) has been found to bind with high affinity to AKAPs, whereas PKA regulatory subunit type I (RI) exhibits much lower affinity for AKAPs[34]. The ratio of between the regulatory subunits RI and RII is important[35–37]. We speculate that TREK-1 may recruit PKA RII subunits and down-regulate the level of the PKA catalytic subunit. Moreover, our data demonstrated TREK-1 increased the activity of GSK-3β and decreased the activity of CREB by reducing the phosphorylation of Akt at Ser473. Subsequently, the cell cycle was halted because of the inhibition of the transcription and translation of cyclin D1 and the promotion of the degradation of cyclin D1. Additionally, *l*-NBP, which is a potent and relatively selective inhibitor of TREK-1, reversed the effect of TREK-1 on cell proliferation; therefore, these findings support our previous research revealing that *l*-NBP promotes neuronal regeneration after ischemic stroke[38].

The regulation of the resting membrane potentials of neurons and the cells of other tissues is among the most vital functions of TREK-1. Previous data from our laboratory demonstrated that, compared with wild-type CHO cells, the resting membrane potential of TREK-1/CHO cells wasdecreased from -17.6 mV to -55.3 mV[19]. Moreover, many studies have demonstrated that the resting membrane potential modulates cell proliferation[39–41], therefore, TREK-1 may control cell proliferation by hyperpolarizing the cell membrane potential.

Although many studies have suggested that inhibiting TREK-1 expression might promote cell proliferation, some authors have reported different results[14, 42]. Specifically, it has been reported that TREK-1 is highly expressed in prostate cancer cells but not in normal prostatic tissues[14]. The causal relationship between TREK-1 expression and cell proliferation in cancer cells is unclear. It is well known that the proliferation mechanisms of cancer cells are different and more complicated than those of normal cells. The proliferation of cancer cells might be promoted factors other than TREK-1. Notably, these authors were unable to directly demonstrate whether TREK-1 promoted tumor cells or whether channel expression was increased by compensation. Furthermore, 3 isoforms of TREK-1 (TREK-1a, TREK-1b, and TREK-1c) have been found, and these isoforms exhibit different N-terminal structures. It is unknown whether there are any functional differences among the isoforms. The TREK-1c variant (426 amino acids) differs in the 5′ UTR and the beginning of the coding region compared with the TREK-1a variant. The TREK-1a isoform is slightly shorter and has a distinct N-terminus compared with the TREK-1c isoform. Voloshyna and colleagues used TREK-1c in their cancer cell and CHO cell study[14].

Additionally, in some cases, TREK-1 has been found to be up-regulated during organ/tissue damage[10, 43–45]. For example, TREK-1 expression is increased in acute cerebral ischemic stroke, and this increase might have a protective role for neuronal cells because enhanced TREK-1 currents may lower the resting membrane potential and reduce the excitability of the cells, consequently reducing energy consumption. Therefore, the increased expression of TREK-1 might be the result of compensation for the pathological condition and may reduce damage to the cells. In contrast, the inhibition of

TREK-1 may promote neurogenesis after tissue damage such as the damage due to stroke[9, 38]. Therefore, TREK-1 is very important for tissue/cell protection and repair.

In conclusion, the present study demonstrated that the overexpression of TREK-1 in CHO cells inhibited the activity of PKA, increased the activity of p38, and consequently inhibited the expression of cyclin D1, which ultimately resulted in cell cycle arrest at G_1/S. However, no correlation was observed between TREK-1 and activated STAT3. Although the regulatory mechanism of TREK-1 and PKA requires further research, the present study demonstrated important mechanisms by which TREK-1 inhibits the cell cycle. TREK-1 might be a drug target to promote neuronal proliferation and tissue recovery from damage.

Acknowledgements

This work was supported by the National Natural Science Foundation of China (No 81373387) and the National Major Special Project on New Drug Innovation of China (No 2012ZX09301002-004 and No 2014ZX09507003-006-003).

Author contribution

Xiao-liang WANG and Man ZHANG designed the research; Man ZHANG, Wei-ping WANG, Hua-jing YIN, and Jiang LI performed the research; Man ZHANG and Wei-ping WANG analyzed the data; Man ZHANG and Xiao-liang WANG wrote the paper.

References

1 Pardo LA. Voltage-gated potassium channels in cell proliferation. Physiology (Bethesda) 2004; 19: 285–92.
2 Talley EM, Solorzano G, Lei Q, Kim D, Bayliss DA. Cns distribution of members of the two-pore-domain (KCNK) potassium channel family. J Neurosci 2001; 21: 7491–505.
3 Chemin J, Patel AJ, Duprat F, Lauritzen I, Lazdunski M, Honore E. A phospholipid sensor controls mechanogating of the K^+ channel TREK-1. EMBO J 2005; 24: 44–53.
4 Heurteaux C, Lucas G, Guy N, El Yacoubi M, Thummler S, Peng XD, *et al.* Deletion of the background potassium channel TREK-1 results in a depression-resistant phenotype. Nat Neurosci 2006; 9: 1134–41.
5 Xi G, Zhang X, Zhang L, Sui Y, Hui J, Liu S, *et al.* Fluoxetine attenuates the inhibitory effect of glucocorticoid hormones on neurogenesis *in vitro* via a two-pore domain potassium channel, TREK-1. Psychopharmacology (Berl) 2011; 214: 747–59.
6 Chen C, Wang L, Rong X, Wang W, Wang X. Effects of fluoxetine on protein expression of potassium ion channels in the brain of chronic mild stress rats. Acta Pharm Sin B 2015; 5: 55–61.
7 Wu X, Liu Y, Chen X, Sun Q, Tang R, Wang W, *et al.* Involvement of TREK-1 activity in astrocyte function and neuroprotection under simulated ischemia conditions. J Mol Neurosci 2013; 49: 499–506.
8 Lu L, Wang W, Peng Y, Li J, Wang L, Wang X. Electrophysiology and pharmacology of tandem domain potassium channel TREK-1 related BDNF synthesis in rat astrocytes. Naunyn Schmiedebergs Arch Pharmacol 2014; 387: 303–12.
9 Li ZB, Zhang HX, Li LL, Wang XL. Enhanced expressions of arachidonic acid-sensitive tandem-pore domain potassium channels in rat experimental acute cerebral ischemia. Biochem Biophys Res Commun 2005; 327: 1163–9.
10 Wang M, Song J, Xiao W, Yang L, Yuan J, Wang W, *et al.* Changes in lipid-sensitive two-pore domain potassium channel TREK-1 expression and its involvement in astrogliosis following cerebral ischemia in rats. J Mol Neurosci 2012; 46: 384–92.
11 Xu X, Pan Y, Wang X. mRNA expression of the lipid and mechano-gated 2P domain K^+ channels during rat brain development. J Neurogenet 2002; 16: 263–9.
12 Hughes S, Magnay J, Foreman M, Publicover SJ, Dobson JP, El Haj AJ. Expression of the mechanosensitive $2PK^+$ channel TREK-1 in human osteoblasts. J Cell Physiol 2006; 206: 738–48.
13 Yang X, Guo P, Li J, Wang W, Xu S, Wang L, *et al.* Functional study of TREK-1 potassium channels during rat heart development and cardiac ischemia using RNAi techniques. J Cardiovasc Pharmacol 2014; 64: 142–50.
14 Voloshyna I, Besana A, Castillo M, Matos T, Weinstein IB, Mansukhani M, *et al.* TREK-1 is a novel molecular target in prostate cancer. Cancer Res 2008; 68: 1197–203.
15 Patel AJ, Honore E, Maingret F, Lesage F, Fink M, Duprat F, *et al.* A mammalian two pore domain mechano-gated S-like K^+ channel. EMBO J 1998; 17: 4283–90.
16 Mathie A, Veale EL. Therapeutic potential of neuronal two-pore domain potassium-channel modulators. Curr Opin Investig Drugs 2007; 8: 555–62.
17 Dong GX, Feng YP. Effects of NBP on ATPase and anti-oxidant enzymes activities and lipid peroxidation in transient focal cerebral ischemic rats. Zhongguo Yi Xue Ke Xue Yuan Xue Bao 2002; 24: 93–7.
18 Zhang Y, Wang L, Li J, Wang XL. 2-(1-Hydroxypentyl)-benzoate increases cerebral blood flow and reduces infarct volume in rats model of transient focal cerebral ischemia. J Pharmacol Exp Ther 2006; 317: 973–9.
19 Ji XC, Zhao WH, Cao DX, Shi QQ, Wang XL. Novel neuroprotectant chiral 3-*n*-butylphthalide inhibits tandem-pore-domain potassium channel TREK-1. Acta Pharmacol Sin 2011; 32: 182–7.
20 Wang W, Zhang M, Li P, Yuan H, Feng N, Peng Y, *et al.* An increased TREK-1-like potassium current in ventricular myocytes during rat cardiac hypertrophy. J Cardiovasc Pharmacol 2013; 61: 302–10.
21 Kim JK, Diehl JA. Nuclear cyclin D1: an oncogenic driver in human cancer. J Cell Physiol 2009; 220: 292–6.
22 Wang W, Zhao Y, Yang J, Lin B, Gu H, Cao X, *et al.* Cyclin D1 polymorphism and oral cancer: a meta-analysis. Mol Biol Rep 2013; 40: 87–95.
23 Tobin NP, Bergh J. Analysis of Cyclin D1 in breast cancer: a call to arms. Curr Breast Cancer Rep 2012; 4: 171–3.
24 Ding GX, Liu J, Feng CC, Jiang HW, Xu JF, Ding Q. Slug regulates Cyclin D1 expression by ubiquitin-proteasome pathway in prostate cancer cells. Panminerva Med 2012; 54: 219–23.
25 Liu J, Liao Q, Zhang Y, Sun S, Zhong C, Liu X. Cyclin D1 G870A polymorphism and lung cancer risk: a meta-analysis. Tumour Biol 2012; 33: 1467–76.
26 Wagner EF, Nebreda AR. Signal integration by JNK and p38 MAPK pathways in cancer development. Nat Rev Cancer 2009; 9: 537–49.
27 Malberg JE, Duman RS. Cell proliferation in adult hippocampus is decreased by inescapable stress: reversal by fluoxetine treatment. Neuropsychopharmacology 2003; 28: 1562–71.
28 Dowlatshahi D, MacQueen GM, Wang JF, Young LT. Increased temporal cortex CREB concentrations and antidepressant treatment in major depression. Lancet 1998; 352: 1754–5.
29 VanArsdale T, Boshoff C, Arndt KT, Abraham RT. Molecular pathways: targeting the Cyclin D-CDK4/6 axis for cancer treatment. Clin Cancer Res 2015; 21: 2905–10.

30 Sanchez-Martinez C, Gelbert LM, Lallena MJ, de Dios A. Cyclin dependent kinase (CDK) inhibitors as anticancer drugs. Bioorg Med Chem Lett 2015; 25: 3420–35.
31 Tsukahara T, Haniu H, Matsuda Y. Cyclic phosphatidic acid induces G_0/G_1 arrest, inhibits AKT phosphorylation, and downregulates cyclin D1 expression in colorectal cancer cells. Cell Mol Biol Lett 2015; 20: 38–47.
32 Densham RM, Todd DE, Balmanno K, Cook SJ. ERK1/2 and p38 cooperate to delay progression through G_1 by promoting cyclin D1 protein turnover. Cell Signal 2008; 20: 1986–94.
33 Sandoz G, Thummler S, Duprat F, Feliciangeli S, Vinh J, Escoubas P, *et al*. AKAP150, a switch to convert mechano-, pH- and arachidonic acid-sensitive TREK K^+ channels into open leak channels. EMBO J 2006; 25: 5864–72.
34 Tortora G, Pepe S, Bianco C, Damiano V, Ruggiero A, Baldassarre G, *et al*. Differential effects of protein kinase A sub-units on Chinese-hamster-ovary cell cycle and proliferation. Int J Cancer 1994; 59: 712–6.
35 Tortora G, Pepe S, Bianco C, Baldassarre G, Budillon A, Clair T, *et al*. The RI alpha subunit of protein kinase A controls serum dependency and entry into cell cycle of human mammary epithelial cells. Oncogene 1994; 9: 3233–40.
36 Tortora G, Budillon A, Yokozaki H, Clair T, Pepe S, Merlo G, *et al*. Retroviral vector-mediated overexpression of the RII beta subunit of the cAMP-dependent protein kinase induces differentiation in human leukemia cells and reverts the transformed phenotype of mouse fibroblasts. Cell Growth Differ 1994; 5: 753–9.
37 Elliott MR, Tolnay M, Tsokos GC, Kammer GM. Protein kinase A regulatory subunit type II beta directly interacts with and suppresses CREB transcriptional activity in activated T cells. J Immunol 2003; 171: 3636–44.
38 Yang LC, Li J, Xu SF, Cai J, Lei H, Liu DM, *et al*. L-3-n-butylphthalide promotes neurogenesis and neuroplasticity in cerebral ischemic rats. CNS Neurosci Ther 2015; 21: 733–41.
39 Lan JY, Williams C, Levin M, Black LD 3rd. Depolarization of cellular resting membrane potential promotes neonatal cardiomyocyte proliferation *in vitro*. Cell Mol Bioeng 2014; 7: 432–45.
40 Jeub M, Herbst M, Spauschus A, Fleischer H, Klockgether T, Wuellner U, *et al*. Potassium channel dysfunction and depolarized resting membrane potential in a cell model of SCA3. Exp Neurol 2006; 201: 182–92.
41 Chilton L, Ohya S, Freed D, George E, Drobic V, Shibukawa Y, *et al*. K^+ currents regulate the resting membrane potential, proliferation, and contractile responses in ventricular fibroblasts and myofibroblasts. Am J Physiol Heart Circ Physiol 2005; 288: H2931–9.
42 Patel SK, Jackson L, Warren AY, Arya P, Shaw RW, Khan RN. A role for two-pore potassium (K2P) channels in endometrial epithelial function. J Cell Mol Med 2013; 17: 134–46.
43 Wu X, Liu Y, Chen X, Sun Q, Tang R, Wang W, *et al*. Involvement of TREK-1 activity in astrocyte function and neuroprotection under simulated ischemia conditions. J Mol Neurosci 2013; 49: 499–506.
44 Wu X, Tang R, Liu Y, Song J, Yu Z, Wang W, *et al*. Small RNA interference-mediated gene silencing of TREK-1 potassium channel in cultured astrocytes. J Huazhong Univ Sci Technolog Med Sci 2012; 32: 849–55.
45 Lin DH, Zhang XR, Ye DQ, Xi GJ, Hui JJ, Liu SS, *et al*. The role of the two-pore domain potassium channel TREK-1 in the therapeutic effects of escitalopram in a rat model of poststroke depression. CNS Neurosci Ther 2015; 21: 504–12.